



# Rotating Neutron Stars

Fridolin Weber and Philip Rosenfield

February 2007

Publication Number: CSRCR2007-06

Computational Science &  
Engineering Faculty and Students  
Research Articles

Database Powered by the  
Computational Science Research Center  
Computing Group

# COMPUTATIONAL SCIENCE & ENGINEERING



**SAN DIEGO STATE  
UNIVERSITY**

Computational Science Research Center  
College of Sciences  
5500 Campanile Drive  
San Diego, CA 92182-1245  
(619) 594-3430



# Rotating Neutron Stars

Fridolin Weber <sup>a</sup> and Philip Rosenfield

Department of Physics, San Diego State University, 5500 Campanile Drive, San Diego, CA 92182-1233, USA

Received: date / Revised version: date

**Abstract.** Because of the tremendous densities that exist in the cores of neutron stars, a significant fraction of the matter in the cores of such stars is likely to exist in the form of hyperons. Depending on spin frequency, the hyperon content changes dramatically in rotating neutron stars, as discussed in this paper.

**PACS.** 26.60 +c Nuclear matter aspects of neutron stars – 97.60.Gb Pulsars – 97.60.Jd Neutron stars

## 1 Introduction

Rotating neutron stars are called pulsars. Three distinct classes of pulsars are currently known. These are (1) rotation-powered pulsars, where the loss of rotational energy of the star powers the emitted electromagnetic radiation, (2) accretion-powered (X-ray) pulsars, where the gravitational potential energy of the matter accreted from a low-mass companion is the energy source, and (3) magnetars, where the decay of a ultra-strong magnetic field powers the radiation. The matter in the cores of rotating neutron stars is compressed to ultra-high densities that may be more than an order of magnitude greater than the density of atomic nuclei. This makes (rotating) neutron stars superb astrophysical laboratories for a wide range of fascinating physical studies [1, 2, 3]. This includes the physics of hyperons in cold ultra-dense matter, whose thresholds, according to model calculations, are easily reached in the cores of neutron stars (see Fig. 1), depending on the mass and rotational frequency of a neutron star. The most rapidly rotating, currently known neutron star is pulsar PSR J1748-2446ad, which rotates at a period of 1.39 ms (which corresponds to a rotational frequency of 719 Hz) [4]. It is followed by PSRs B1937+21 [5] and B1957+20 [6] whose rotational periods are 1.58 ms (633 Hz) and 1.61 ms (621 Hz), respectively. Finally, we mention the recent discovery of X-ray burst oscillations from the neutron star X-ray transient XTE J1739-285 [7], which could suggest that XTE J1739-285 contains the most rapidly rotating neutron star yet discovered. Rapid rotation changes the structure and composition of neutron stars dramatically, and leads to novel phenomena like frame dragging (Lense Thirring effect), as discussed in this paper.

<sup>a</sup> The research of F. Weber is supported by the National Science Foundation under Grant PHY-0457329, and by the Research Corporation.

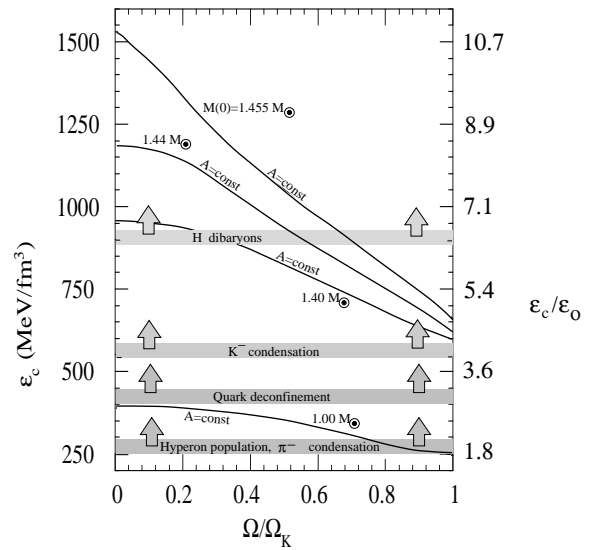


**Fig. 1.** Change of central density with rotational neutron star frequency [2].  $\epsilon_0 = 140 \text{ MeV/fm}^3$  denotes the density of nuclear matter,  $\Omega_K$  is the Kepler frequency, and  $M(0)$  is the star's mass at zero rotation.

## 2 Stellar structure equations

Since neutron stars are objects of highly compressed matter, the geometry of spacetime is changed dramatically from flat space by these objects. Neutron star models are thus to be computed from Einstein's field equations of general relativity ( $\mu, \nu=0,1,2,3$ ),

$$G_{\mu\nu} \equiv R_{\mu\nu} - \frac{1}{2}g_{\mu\nu}R = 8\pi T_{\mu\nu}(\epsilon, P(\epsilon)), \quad (1)$$

which couples Einstein's curvature tensor,  $G_{\mu\nu}$ , to the energy-momentum density tensor,  $T_{\mu\nu}$ , of the stellar matter. The quantities  $R_{\mu\nu} \equiv \Gamma_{\mu\sigma;\nu}^{\sigma} - \Gamma_{\mu\nu;\sigma}^{\sigma} + \Gamma_{\kappa\nu}^{\sigma}\Gamma_{\mu\sigma}^{\kappa} - \Gamma_{\kappa\sigma}^{\sigma}\Gamma_{\mu\nu}^{\kappa}$ ,  $g_{\mu\nu}$ , and  $R \equiv R_{\mu\nu}g^{\mu\nu}$  in denote the Ricci tensor, metric tensor and scalar curvature, respectively [2].

(Commas followed by a Greek letter denote derivatives with respect to space-time coordinates, e.g.  $_{,\nu} = \partial/\partial x^\nu$ .) The Christoffel symbols are defined as  $\Gamma_{\mu\nu}^\sigma = (1/2)g^{\sigma\lambda}(g_{\mu\lambda,\nu} + g_{\nu\lambda,\mu} - g_{\mu\nu,\lambda})$ . Theories of superdense matter enter in Eq. (1) through the energy–momentum tensor,

$$T_{\mu\nu} = u_\mu u_\nu (\epsilon + P) + g_{\mu\nu} P, \quad (2)$$

which contains the equation of state (EoS), i.e. pressure as a function on energy density,  $P(\epsilon)$ , of the stellar matter. The quantities  $u_\mu$  and  $u_\nu$  in Eq. (2) are four-velocities, defined as  $u_\mu = dx_\mu/d\tau$  and  $u_\nu = dx_\nu/d\tau$ , where  $d\tau^2 = -ds^2$ . These velocities are the components of the macroscopic velocity of the stellar matter with respect to the actual coordinate system that is being used.

## 2.1 Non-rotating stars

Non-rotating neutron stars are spherically symmetric. The metric of such stars thus depends only on the radial coordinate and is given by

$$ds^2 = -e^{2\Phi} dt^2 + e^{2\Lambda} dr^2 + r^2 d\theta^2 + r^2 \sin^2\theta d\phi^2, \quad (3)$$

where  $\Phi$  and  $\Lambda$  are the radially varying metric functions. From Eq. (3) it follows that the components of the metric tensor are given by

$$g_{tt} = -e^{2\Phi}, \quad g_{rr} = e^{2\Lambda}, \quad g_{\theta\theta} = r^2, \quad g_{\phi\phi} = r^2 \sin^2\theta, \quad (4)$$

so that the only non-vanishing Christoffel symbols are

$$\begin{aligned} \Gamma_{tt}^r &= e^{2\Phi-2\Lambda}\Phi', & \Gamma_{tr}^t &= \Phi', & \Gamma_{rr}^r &= \Lambda', & \Gamma_{r\theta}^\theta &= r^{-1}, \\ \Gamma_{r\phi}^\phi &= r^{-1}, & \Gamma_{\theta\theta}^r &= -re^{-2\Lambda}, & \Gamma_{\theta\phi}^\phi &= \frac{\cos\theta}{\sin\theta}, \\ \Gamma_{\phi\phi}^r &= -r\sin^2\theta e^{-2\Lambda}, & \Gamma_{\phi\phi}^\theta &= -\sin\theta \cos\theta. \end{aligned} \quad (5)$$

Substituting Eqs. (4) and (5) into (1) and using  $T_{\mu\nu;\mu} = 0$  (the semicolon denotes covariant differentiation) leads to the Tolman–Oppenheimer–Volkoff (TOV) equation [2],

$$\frac{dP}{dr} = -\frac{\epsilon m}{r^2} \frac{(1 + P/\epsilon)(1 + 4\pi r^3 P/m)}{1 - 2m/r}, \quad (6)$$

applicable to compact stellar configurations in general relativistic hydrostatic equilibrium. We use units for which the gravitational constant and velocity of light are  $G = c = 1$  so that the mass of the sun is  $M_\odot = 1.47$  km. The mass contained in a sphere of radius  $r$  is given by  $m = 4\pi \int_0^r r'^2 \epsilon dr'$ . Hence the star's total mass follows as  $M \equiv m(R)$ , where  $R$  denotes the star's radius. The Newtonian limit of Eq. (6) is obtained for  $P/\epsilon \ll 1$ ,  $4\pi r^3 P/m \ll 1$ , and  $2m/r \ll 1$ . General relativity, thus, increases the pressure gradient inside the star which leads to smaller, more compact stars. The masses of neutron stars lie between about one and two solar masses, and their radii are around 10 km. Thus,  $2M/R \sim 30 - 60\%$  for neutron stars. Solutions of the TOV equations are shown in Fig. 2.

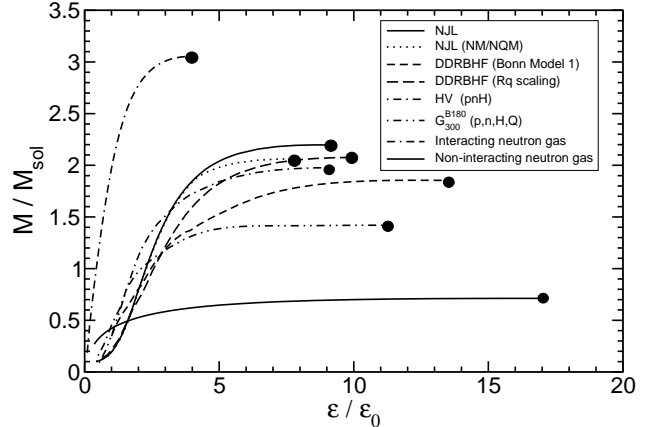


**Fig. 2.** Neutron star mass versus central energy density for different equations of state of neutron star matter [8].

## 2.2 Rotating stars

The structure equations of rotating neutron stars are considerably more complicated than those of non-rotating neutron stars [2]. These complications have their cause in the rotational deformation, that is, a flattening at the pole accompanied by a radial expansion in the equatorial direction, which leads to a dependence of the star's metric on the polar coordinate,  $\theta$ . Secondly, rotation stabilizes a neutron star against gravitational collapse. A rotating neutron star can therefore carry more mass than a non-rotating star. Being more massive, however, means that

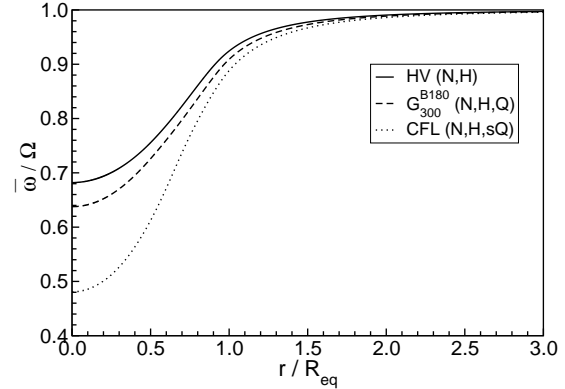


**Fig. 3.** Dragging of local inertial frames (Lense-Thirring effect) caused by  $\sim 1.4 M_\odot$  neutron stars rotating at 2 ms [9]. The frequency  $\bar{\omega}$  is defined in Eq. (9).

the geometry of space-time is changed too. This renders the metric functions of a rotating neutron star frequency dependent. Finally, the general relativistic effect of the dragging of local inertial frames implies the occurrence of an additional non-diagonal term,  $g^{t\phi}$ , in the metric tensor  $g^{\mu\nu}$ . This term imposes a self-consistency condition on the stellar structure equations, since the degree at which the local inertial frames are dragged along by the star is de-

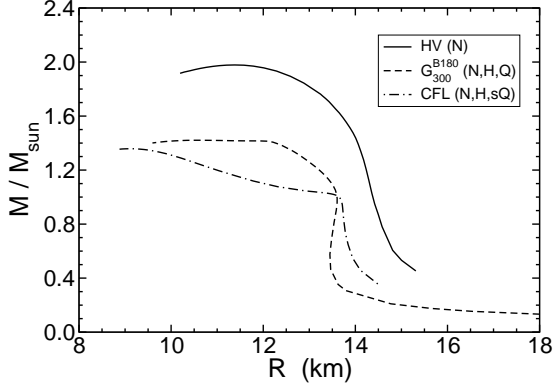


**Fig. 4.** Mass–radius relations of non-rotating neutron stars for different EoSs.

terminated by the initially unknown stellar properties like mass and rotational frequency. The covariant components of the metric tensor of a rotating compact star are thus given by [2, 10]

$$\begin{aligned} g_{tt} &= -e^{2\nu} + e^{2\psi}\omega^2, & g_{t\phi} &= -e^{2\psi}\omega, & g_{rr} &= e^{2\lambda}, \\ g_{\theta\theta} &= e^{2\mu}, & g_{\phi\phi} &= e^{2\psi}, \end{aligned} \quad (7)$$

which corresponds to a line element,  $ds^2 = g_{\mu\nu}dx^\mu dx^\nu$ , of the form

$$ds^2 = -e^{2\nu}dt^2 + e^{2\psi}(d\phi - \omega dt)^2 + e^{2\mu}d\theta^2 + e^{2\lambda}dr^2. \quad (8)$$

Here each metric function, i.e.  $\nu$ ,  $\psi$ ,  $\mu$  and  $\lambda$ , as well as the angular velocities of the local inertial frames,  $\omega$ , depend on the radial coordinate  $r$  and on the polar angle  $\theta$  and, implicitly, on the star’s angular velocity  $\Omega$ . Of particular interest is the relative angular frame dragging frequency,  $\bar{\omega}$ , defined as

$$\bar{\omega}(r, \theta, \Omega) \equiv \Omega - \omega(r, \theta, \Omega), \quad (9)$$

which is the angular velocity of the star,  $\Omega$ , relative to the angular velocity of a local inertial frame,  $\omega$ . It is this frequency that is of relevance when discussing the rotational flow of the fluid inside the star, since the magnitude of the centrifugal force acting on a fluid element is governed—in general relativity as well as in Newtonian gravitational theory—by the rate of rotation of the fluid element relative to a local inertial frame [11]. In contrast to Newtonian theory, however, the inertial frames inside (and outside) a general relativistic fluid are not at rest with respect to the distant stars. Rather, the local inertial frames are dragged along by the rotating fluid. Depending on the internal stellar constitution, this effect can be quite strong, as shown in Fig. 3 for neutron stars rotating at 2 ms [9]. The stellar models are computed for three different equations of state: (1) HV, which describes neutron stars made of nucleons (N) and hyperons (H);  $G_{300}^{B180}$ , which describes neutron star matter in terms of nucleons, hyperons, and quarks (Q); and CFL, which assumes that the quarks are color superconducting (CFL phase) [12]. For a very compact neutron star, as obtained for the CFL

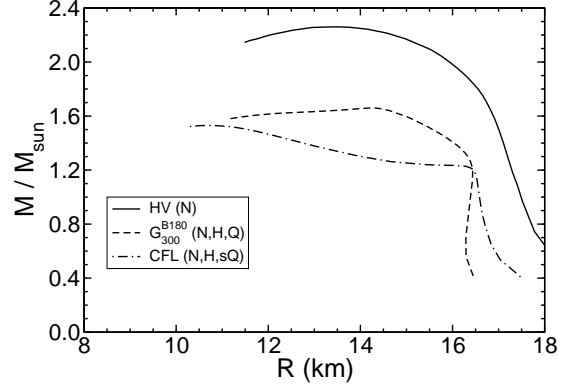


**Fig. 5.** Same as Fig. 4, but for neutron stars rotating at the mass shedding (Kepler) frequency.

case, one sees that the local inertial frames at the star’s center rotate at about half the star’s rotational frequency,  $\omega(r=0) \simeq \Omega/2$ . This value drops to about 15% for the local inertial frames located at the star’s equator.

Figures 4 and 5 show the influence of rotation on the mass–radius relationship of neutron stars. For ultrafast rotation at the Kepler frequency, a mass increase up to  $\sim 20\%$  is obtained, depending on the equation of state. The equatorial radius increases by several kilometers, while the polar radius get smaller by several kilometers. The ratio between both radii is around  $2/3$ , except for rotation close to the Kepler frequency.

### 2.3 Limiting rotational periods

No simple stability criteria are known for rapidly rotating stellar configurations in general relativity. However, an absolute limit on rapid rotation is set by the onset of mass shedding from the equator of a rotating star. The corresponding rotational frequency is known as the Kepler frequency,  $\Omega_K$ . In classical mechanics, the expression for the Kepler frequency, determined by the equality between the centrifugal force and gravity, is readily obtained as  $\Omega_K = \sqrt{M/R^3}$ . In order to derive the general relativistic counterpart of this relation, one applies the extremal principle to the circular orbit of a point mass rotating at the star’s equator. Since  $r = \theta = \text{const}$  for a point mass there, one has  $dr = d\theta = 0$ . The line element (8) then reduces to  $ds^2 = (e^{2\nu} - e^{2\psi}(\Omega - \omega)^2) dt^2$ . Substituting this expression into  $J \equiv \int_{s_1}^{s_2} ds$ , where  $s_1$  and  $s_2$  refer to points located at that particular orbit for which  $J$  becomes extremal, gives

$$J = \int_{s_1}^{s_2} dt \sqrt{e^{2\nu} - e^{2\psi}(\Omega - \omega)^2}. \quad (10)$$

Applying the extremal condition  $\delta J = 0$  to Eq. (10) and noticing that  $V = e^{\psi-\nu}(\Omega - \omega)$  then leads to

$$\psi_{,r} e^{2\nu} V^2 - \omega_{,r} e^{\nu+\psi} V - \nu_{,r} e^{2\nu} = 0. \quad (11)$$

This relation constitutes a quadratic equation for the orbital velocity  $V$  of a particle at the star’s equator. One

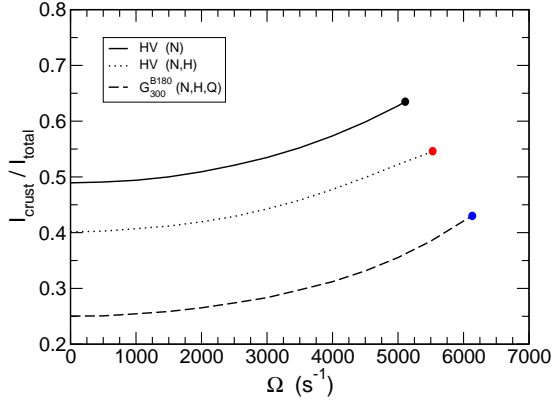


Fig. 6. Moment of inertia of several sample neutron stars.

thus obtains for the Kepler frequency  $\Omega_K$  the final relation [2]

$$\Omega_K = \omega + \frac{\omega_{,r}}{2\psi_{,r}} + e^{\nu-\psi} \sqrt{\frac{\nu_{,r}}{\psi_{,r}} + \left(\frac{\omega_{,r}}{2\psi_{,r}} e^{\psi-\nu}\right)^2}, \quad (12)$$

which is to be solved self-consistently at the equator of a rotating neutron star. The general relativistic Kepler period follows from Eq. (12) as  $P_K = 2\pi/\Omega_K$ . For typical neutron star matter equations of state, the Kepler period obtained for  $1.4 M_\odot$  neutron stars scatters around 1 ms. One exception to this are strange quark matter stars. These are self-bound and, thus, tend to possess smaller radii than conventional neutron stars, which are bound by gravity only. Because of their smaller radii, strange stars can withstand mass shedding down to periods of around 0.5 ms [13, 14]. The CFL neutron star discussed just above is a quark-hybrid star and as such bound by gravity only. The dense quark core in the center of this neutron star implies a relatively large binding energy of  $0.12 M_\odot$ , leading to a rather low mass shedding period of 0.7 ms. In closing this section, we introduce the moment of inertia of a rotating neutron star described by the metric in Eq. (8). For such stars the moment of inertia is given by

$$I = 2\pi \int_0^\pi d\theta \int_0^{R(\theta)} dr e^{\lambda+\mu+\nu+\psi} \frac{\epsilon + P}{e^{2\nu-2\psi} - \bar{\omega}^2} \frac{\bar{\omega}}{\Omega}. \quad (13)$$

Figure 6 shows that the crustal fraction of the moment of inertia of a neutron star may be around 50% smaller if the star contains a very soft phase of matter like CFL quark matter. This may be of relevance for pulsar glitch models and the modeling of the post-glitch behavior of pulsars.

### 3 Composition of neutron star matter

A vast number of models for the equation of state of neutron star matter has been derived in the literature over the years. These models can roughly be classified as follows:

- Thomas-Fermi based models [15, 16]

- Schroedinger-based models (e.g. variational approach, Monte Carlo techniques, hole line expansion (Brueckner theory), coupled cluster method, Green function method) [17, 18, 19, 20]
- Relativistic field-theoretical treatments (relativistic mean field (RMF), Hartree-Fock (RHF), standard Brueckner-Hartree-Fock (RBHF), density dependent RBHF (DD-RBHF) [1, 21, 22, 23, 24, 25, 26]
- Nambu-Jona-Lasinio (NJL) models [27, 28, 29, 30, 31, 32]
- Chiral SU(3) quark mean field model [33].

Neutron star masses computed for some of these models are shown in Fig. 2.

#### 3.1 Relativistic nuclear field-theoretical models

Relativistic nuclear field-theoretical models [1, 2, 21, 22, 23, 24, 25, 26] are based on Lagrangians of the form  $\mathcal{L} = \mathcal{L}_B + \mathcal{L}_M + \mathcal{L}_{int} + \mathcal{L}_{lept}$ , where

$$\mathcal{L}_B = \sum_B \bar{\psi}_B (i\gamma_\mu \partial^\mu - m_B) \psi_B, \quad (14)$$

$$\mathcal{L}_M = \frac{1}{2} \sum_{i=\sigma,\delta} (\partial_\mu \Phi_i \partial^\mu \Phi_i - m_i^2 \Phi_i^2) - \frac{1}{2} \sum_{\kappa=\omega,\rho} \left( \frac{1}{2} F_{\mu\nu}^{(\kappa)} F^{(\kappa)\mu\nu} - m_\kappa^2 A_\mu^{(\kappa)} A^{(\kappa)\mu} \right), \quad (15)$$

$$\mathcal{L}_{int} = \bar{\psi} \hat{\Gamma}_\sigma(\bar{\psi}, \psi) \psi \Phi_\sigma - \bar{\psi} \hat{\Gamma}_\omega(\bar{\psi}, \psi) \gamma_\mu \psi A^{(\omega)\mu} + \bar{\psi} \hat{\Gamma}_\delta(\bar{\psi}, \psi) \boldsymbol{\tau} \psi \boldsymbol{\Phi}_\delta - \bar{\psi} \hat{\Gamma}_\rho(\bar{\psi}, \psi) \gamma_\mu \boldsymbol{\tau} \psi \mathbf{A}^{(\rho)\mu}. \quad (16)$$

Here,  $\mathcal{L}_B$  and  $\mathcal{L}_M$  are the free baryonic and the free mesonic Lagrangians, respectively, and interactions are described by  $\mathcal{L}_{int}$ , where  $F_{\mu\nu}^{(\kappa)} = \partial_\mu A_\nu^{(\kappa)} - \partial_\nu A_\mu^{(\kappa)}$  is the field strength tensor of one of the vector mesons ( $\kappa = \omega, \rho$ ). In the case of RMF, RHF and RBHF the meson-baryon vertices  $\hat{\Gamma}_\alpha$  ( $\alpha = \sigma, \omega, \delta, \rho$ ) are density-independent quantities which are given by expressions like  $\hat{\Gamma}_\sigma = ig_\sigma$  for the scalar  $\sigma$  meson,  $\hat{\Gamma}_\omega^\mu = g_\omega \gamma^\mu + (i/2)(f_\omega/2m)\partial_\lambda[\gamma^\lambda, \gamma^\mu]$  for  $\omega$  mesons, etc. [2]. In the framework of the DD-RBHF scheme, the meson-baryon vertices  $\hat{\Gamma}_\alpha$  depend on the baryon field operators  $\psi$  [24]. The field equations that follow from Eqs. (14)–(16) have the mathematical form

$$(i\gamma^\mu \partial_\mu - m_B) \psi_B(x) = \sum_{M=i,\kappa} M(x) \hat{\Gamma}_M \psi_B(x), \quad (17)$$

$$(\partial^\mu \partial_\mu + m_\sigma^2) \sigma(x) = \sum_B \bar{\psi}_B(x) \hat{\Gamma}_\sigma \psi_B(x), \quad (18)$$

plus similar equations for the other mesons [2, 24].

#### 3.2 Hyperons and baryon resonances

At the densities in the interior of neutron stars, the neutron chemical potential,  $\mu^n$ , is likely to exceed the masses, modified by interactions, of  $\Sigma$ ,  $\Lambda$  and possibly  $\Xi$  hyperons [2, 34]. Hence, in addition to nucleons, neutron star

matter may be expected to contain significant populations of strangeness carrying hyperons [34]. The thresholds of the lightest baryon resonances ( $\Delta^-$ ,  $\Delta^0$ ,  $\Delta^+$ ,  $\Delta^{++}$ ) are reached for relativistic mean-field (RMF) calculations

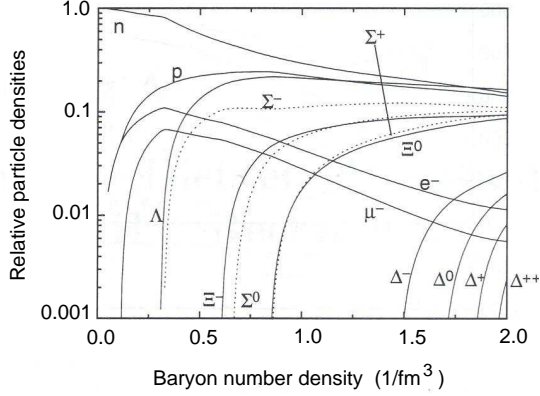


**Fig. 7.** Composition of neutron star matter in RMF.

at densities which correspond to unstable neutron stars. This is different for relativistic Brueckner-Hartree-Fock (RBHF) calculations where  $\Delta$ 's appear rather abundantly

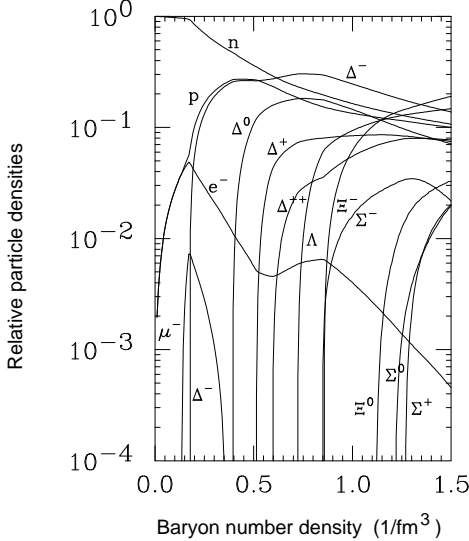


**Fig. 8.** Same as Fig. 7, but computed in RBHF [35].

in stable neutron stars [35], compare Figs. 7 and 8. Depending on the star mass and rotational frequency, the total hyperon population in neutron stars can be very large [34], which is illustrated graphically in Figs. 9–12 for rotating neutron stars based on equations of state computed in the framework of the DD-RBHF formalism. The stars shown in these figures have rotational frequencies ranging from zero to the mass shedding frequency,  $\nu_K$ . Pure neutron matter, therefore, constitutes an excited state relative to hyperonic matter which would quickly transform

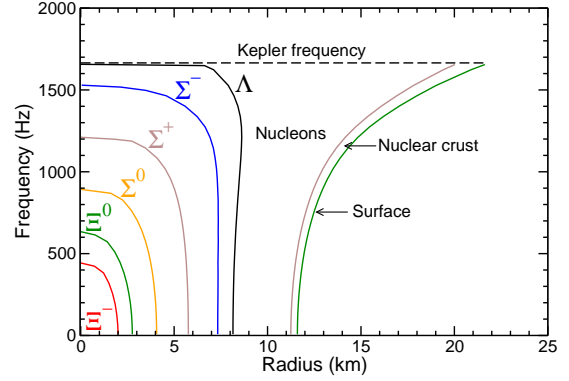


**Fig. 9.** Hyperon composition of a rotating neutron star in equatorial direction. (DD-RBHF calculation performed for Bonn (model 1) potential, non-rotating star mass is  $1.70 M_\odot$ .)

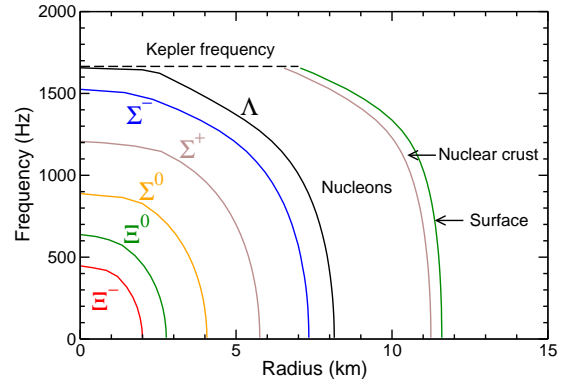
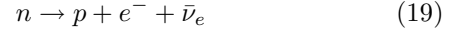


**Fig. 10.** Same as Fig. 9, but in polar direction.

via weak reactions like



to the lower energy state. The chemical potentials associated with reaction (19) in equilibrium obey the relation

$$\mu^n = \mu^p + \mu^{e^-}, \quad (20)$$

where  $\mu^{\bar{\nu}_e} = 0$  since the mean free path of (anti) neutrinos is much smaller than the radius of neutron stars. Hence (anti) neutrinos do not accumulate inside neutron stars. This is different for hot proto-neutron stars [36]. Equation (20) is a special case of the general relation

$$\mu^\chi = B^\chi \mu^n - q^\chi \mu^{e^-}, \quad (21)$$

which holds in any system characterized by two conserved charges. These are in the case of neutron star matter electric charge,  $q^\chi$ , and baryon number charge,  $B^\chi$ . Application of Eq. (21) to the  $\Lambda$  hyperon ( $B^\Lambda = 1$ ,  $q^\Lambda = 0$ ), for instance, leads to  $\mu^\Lambda = \mu^n$ . Ignoring particle interactions, the chemical potential of a relativistic particle of type  $\chi$  is given by  $\mu^\chi = \omega(k_{F_\chi}) \equiv \sqrt{m_\chi^2 + k_{F_\chi}^2}$ , where  $\omega(k_{F_\chi})$  is the single-particle energy of the particle and  $k_{F_\chi}$  its Fermi



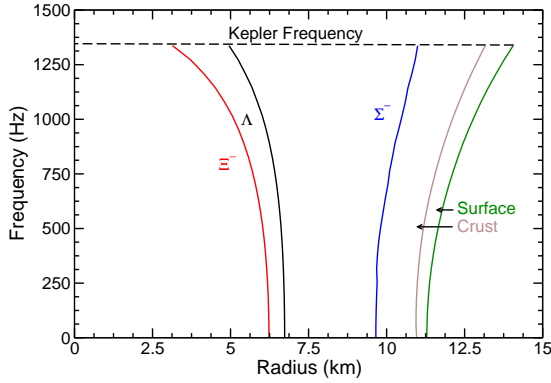


**Fig. 11.** Hyperon composition of a rotating neutron star in equatorial direction. (DD-RBHF calculation performed for Groningen potential, non-rotating star mass is  $1.60 M_{\odot}$ .)

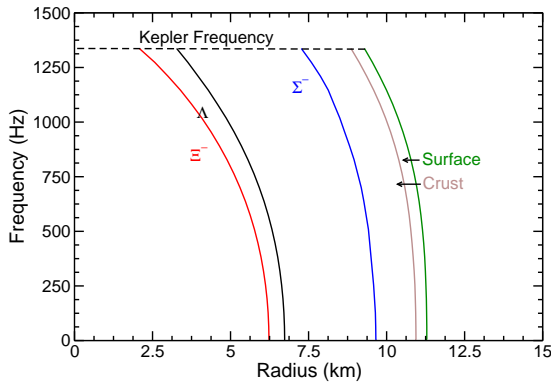


**Fig. 12.** Same as Fig. 9, but in polar direction.

momentum. One thus obtains

$$k_{F_n} \geq \sqrt{m_{\Lambda}^2 - m_n^2} \simeq 3 \text{ fm}^{-1} \Rightarrow n \equiv \frac{k_{F_n}^3}{3\pi^2} \simeq 2n_0, \quad (22)$$

where  $m_{\Lambda} = 1116 \text{ MeV}$  and  $m_n = 939 \text{ MeV}$  was used. That is, if interactions among the particles are ignored, neutrons are replaced with  $\Lambda$ 's in neutron star matter at densities as low as two times the density of nuclear matter. This result is only slightly altered by the inclusion of particle interactions [34]. Densities of just  $\sim 2n_0$  are easily reached in the cores of neutron stars. Neutron stars may thus be expected to contain considerable populations of  $\Lambda$ 's,  $\Sigma$ 's and  $\Xi$ 's, as confirmed by the outcome of DD-RBHF calculations shown graphically above. Depending on the star's mass, the total hyperon population can be very large [34].

## References

1. N. K. Glendenning, *Compact Stars, Nuclear Physics, Particle Physics, and General Relativity*, 2nd ed. (Springer-Verlag, New York, 2000).
2. F. Weber, *Pulsars as Astrophysical Laboratories for Nuclear and Particle Physics*, High Energy Physics, Cosmology and Gravitation Series (IOP Publishing, Bristol, Great Britain, 1999).
3. *Physics of Neutron Star Interiors*, ed. by D. Blaschke, N. K. Glendenning, and A. Sedrakian, Lecture Notes in Physics **578** (Spring-Verlag, Berlin, 2001).
4. J. W. T. Hessels, S. M. Ransom, I. H. Stairs, P. C. C. Freire, V. M. Kaspi, and F. Camilo, *Science* **311** (2006) 1901.
5. D. C. Backer, S. R. Kulkarni, C. Heiles, M. M. Davis, and W. M. Goss, *Nature* **300** (1982) 615.
6. A. S. Fruchter, D. R. Stinebring, and J. H. Taylor, *Nature* **334** (1988) 237.
7. P. Kaaret *et al.*, *Discovery of 1122 Hz X-Ray Burst Oscillations from the Neutron-Star X-Ray Transient XTE J1739-285*, *astro-ph/0611716*.
8. F. Weber, R. Negreiros, P. Rosenfield, and M. Stejner, *Pulsars as astrophysical laboratories for nuclear and particle physics*, to appear in *Prog. Part. Nucl. Phys.* (2007).
9. F. Weber, *Prog. Part. Nucl. Phys.* **54** (2005) 193, (*astro-ph/0407155*).
10. J. L. Friedman, J. R. Ipser, and L. Parker, *Astrophys. J.* **304** (1986) 115.
11. J. B. Hartle, *Astrophys. J.* **150** (1967) 1005.
12. M. Alford, C. Kouvaris, and K. Rajagopal, *Phys. Rev. Lett.* **92** (2004) 222001.
13. N. K. Glendenning and F. Weber, *Astrophys. J.* **400** (1992) 647.
14. N. K. Glendenning, *Phys. Rev. D* **46** (1992) 4161.
15. W. D. Myers and W. J. Swiatecki, *Nucl. Phys.* **A601** (1996) 141.
16. K. Strobel, F. Weber, M. K. Weigel, and Ch. Schaab, *Int. J. Mod. Phys. E* **6**, No. 4 (1997) 669.
17. H. Heiselberg and V. Pandharipande, *Ann. Rev. Nucl. Part. Sci.* **50** (2000) 481.
18. V. R. Pandharipande and R. B. Wiringa, *Rev. Mod. Phys.* **51** (1979) 821.
19. R. B. Wiringa, V. Fiks, and A. Fabrocini, *Phys. Rev. C* **38** (1988) 1010.
20. A. Akmal, V. R. Pandharipande, and D. G. Ravenhall, *Phys. Rev. C* **58** (1998) 1804.
21. H. Lenske and C. Fuchs, *Phys. Lett.* **345B** (1995) 355.
22. C. Fuchs, H. Lenske, and H. H. Wolter, *Phys. Rev. C* **52** (1995) 3043.
23. S. Typel and H. H. Wolter, *Nucl. Phys.* **A656** (1999) 331.
24. F. Hofmann, C. M. Keil, and H. Lenske, *Phys. Rev. C* **64** (2001) 034314.
25. T. Nikšić, D. Vretenar, P. Finelli and P. Ring, *Phys. Rev. C* **66** (2002) 024306.
26. S. F. Ban, J. Li, S. Q. Zhang, H. Y. Jia, and J. P. Sang, and J. Meng, *Phys. Rev. C* **69** (2004) 045805.
27. M. Buballa, *Phys. Rept.* **407** (2005) 205.
28. D. Blaschke, S. Fredriksson, H. Grigorian, A. M. Öztas and F. Sandin, *Phys. Rev. D* **72** (2005) 065020.
29. S. B. Ruster, V. Werth, M. Buballa, I. A. Shovkovy, and D. H. Rischke, *Phys. Rev. D* **72** (2005) 034004.
30. H. Abuki and T. Kunihiro, *Nucl. Phys. A* **768** (2006) 118.
31. S. Lawley, W. Bentz, and A. W. Thomas, *J. Phys. G: Nucl. Part. Phys.* **32** (2006) 667.
32. S. Lawley, W. Bentz, and A. W. Thomas, *Phys. Lett.* **B632** (2006) 495.
33. P. Wang, S. Lawley, D. B. Leinweber, A. W. Thomas, and A. G. Williams, *Phys. Rev. C* **72** (2005) 045801.
34. N. K. Glendenning, *Astrophys. J.* **293** (1985) 470.
35. H. Huber, F. Weber, M. K. Weigel, and Ch. Schaab, *Int. J. Mod. Phys. E* **7**, No. 3 (1998) 301.
36. M. Prakash, I. Bombaci, M. Prakash, P. J. Ellis, J. M. Lattimer, and R. Knorren, *Phys. Rep.* **280** (1997) 1.